TNF-α production and inhibits NO secretion by engaging scavenger receptors. Microb. Pathog. *50*, 350–359.

Koppel, E.A., Ludwig, I.S., Hernandez, M.S., Lowary, T.L., Gadikota, R.R., Tuzikov, A.B., Vandenbroucke-Grauls, C.M., van Kooyk, Y., Appelmelk, B.J., and Geijtenbeek, T.B. (2004). Identification of the mycobacterial carbohydrate structure that binds the C-type lectins DC-SIGN, L-SIGN and SIGNR1. Immunobiology *209*, 117–127.

Lee, W.B., Kang, J.S., Yan, J.J., Lee, M.S., Jeon, B.Y., Cho, S.N., and Kim, Y.J. (2012). Neutrophils promote mycobacterial trehalose dimycolate-induced lung inflammation via the Mincle pathway. PLoS Pathog. *8*, e1002614.

LeibundGut-Landmann, S., Gross, O., Robinson, M.J., Osorio, F., Slack, E.C., Tsoni, S.V., Schweighoffer, E., Tybulewicz, V., Brown, G.D., Ruland, J., and Reis e Sousa, C. (2007). Syk- and CARD9-dependent coupling of innate immunity to the induction of T helper cells that produce interleukin 17. Nat. Immunol. *8*, 630–638.

Leopold, K., and Fischer, W. (1993). Molecular analysis of the lipoglycans of *Mycobacterium tuberculosis*. Anal. Biochem. *208*, 57–64.

Maglione, P.J., Xu, J., Casadevall, A., and Chan, J. (2008). Fc γ receptors regulate immune activation and susceptibility during *Mycobacterium tuberculosis* infection. J. Immunol. *180*, 3329–3338.

Mazurek, J., Ignatowicz, L., Kallenius, G., Svenson, S.B., Pawlowski, A., and Hamasur, B. (2012). Divergent effects of mycobacterial cell wall glycolipids on maturation and function of human monocyte-derived dendritic cells. PLoS ONE *7*, e42515.

McGreal, E.P., Rosas, M., Brown, G.D., Zamze, S., Wong, S.Y., Gordon, S., Martinez-Pomares, L., and Taylor, P.R. (2006). The carbohydrate-recognition domain of Dectin-2 is a C-type lectin with specificity for high mannose. Glycobiology *16*, 422–430.

Mishra, A.K., Driessen, N.N., Appelmelk, B.J., and Besra, G.S. (2011). Lipoarabinomannan and related glycoconjugates: structure, biogenesis and role in *Mycobacterium tuberculosis* physiology and host-pathogen interaction. FEMS Microbiol. Rev. *35*, 1126–1157.

Miyake, Y., Toyonaga, K., Mori, D., Kakuta, S., Hoshino, Y., Oyamada, A., Yamada, H., Ono, K.I., Suyama, M., Iwakura, Y., et al. (2013). C-type lectin MCL is an FcRγ-coupled receptor that mediates the adjuvanticity of mycobacterial cord factor. Immunity *38*, 1050–1062.

Nagaoka, K., Takahara, K., Minamino, K., Takeda, T., Yoshida, Y., and Inaba, K. (2010). Expression of C-type lectin, SIGNR3, on subsets of dendritic cells, macrophages, and monocytes. J. Leukoc. Biol. *88*, 913–924.

Nigou, J., Zelle-Rieser, C., Gilleron, M., Thurnher, M., and Puzo, G. (2001). Mannosylated lipoarabinomannans inhibit IL-12 production by human dendritic cells: evidence for a negative signal delivered through the mannose receptor. J. Immunol. *166*, 7477–7485.

O'Garra, A., Redford, P.S., McNab, F.W., Bloom, C.I., Wilkinson, R.J., and Berry, M.P. (2013). The immune response in tuberculosis. Annu. Rev. Immunol. *31*, 475–527.

Pieters, J. (2008). *Mycobacterium tuberculosis* and the macrophage: maintaining a balance. Cell Host Microbe *3*, 399–407.

Pitarque, S., Herrmann, J.L., Duteyrat, J.L., Jackson, M., Stewart, G.R., Lecointe, F., Payre, B., Schwartz, O., Young, D.B., Marchal, G., et al. (2005). Deciphering the molecular bases of *Mycobacterium tuberculosis* binding to the lectin DC-SIGN reveals an underestimated complexity. Biochem. J. *392*, 615–624.

Redford, P.S., Murray, P.J., and O'Garra, A. (2011). The role of IL-10 in immune regulation during *M. tuberculosis* infection. Mucosal Immunol. *4*, 261–270.

Richmond, J.M., Lee, J., Green, D.S., Kornfeld, H., and Cruikshank, W.W. (2012). Mannose-capped lipoarabinomannan from *Mycobacterium tuberculosis* preferentially inhibits sphingosine-1-phosphate-induced migration of Th1 cells. J. Immunol. *189*, 5886–5895.

Robinson, M.J., Osorio, F., Rosas, M., Freitas, R.P., Schweighoffer, E., Gross, O., Verbeek, J.S., Ruland, J., Tybulewicz, V., Brown, G.D., et al. (2009). Dectin-2 is a Syk-coupled pattern recognition receptor crucial for Th17 responses to fungal infection. J. Exp. Med. *206*, 2037–2051.

Saijo, S., Ikeda, S., Yamabe, K., Kakuta, S., Ishigame, H., Akitsu, A., Fujikado, N., Kusaka, T., Kubo, S., Chung, S.H., et al. (2010). Dectin-2 recognition of α-mannans and induction of Th17 cell differentiation is essential for host defense against *Candida albicans*. Immunity *32*, 681–691.

Sato, K., Yang, X.L., Yudate, T., Chung, J.S., Wu, J., Luby-Phelps, K., Kimberly, R.P., Underhill, D., Cruz, P.D., Jr., and Ariizumi, K. (2006). Dectin-2 is a pattern recognition receptor for fungi that couples with the Fc receptor γ chain to induce innate immune responses. J. Biol. Chem. *281*, 38854–38866.

Schlesinger, L.S., Hull, S.R., and Kaufman, T.M. (1994). Binding of the terminal mannosyl units of lipoarabinomannan from a virulent strain of *Mycobacterium tuberculosis* to human macrophages. J. Immunol. *152*, 4070–4079.

Tailleux, L., Schwartz, O., Herrmann, J.L., Pivert, E., Jackson, M., Amara, A., Legres, L., Dreher, D., Nicod, L.P., Gluckman, J.C., et al. (2003). DC-SIGN is the major *Mycobacterium tuberculosis* receptor on human dendritic cells. J. Exp. Med. *197*, 121–127.

Tanne, A., Ma, B., Boudou, F., Tailleux, L., Botella, H., Badell, E., Levillain, F., Taylor, M.E., Drickamer, K., Nigou, J., et al. (2009). A murine DC-SIGN homologue contributes to early host defense against *Mycobacterium tuberculosis*. J. Exp. Med. *206*, 2205–2220.

Torrelles, J.B., Azad, A.K., and Schlesinger, L.S. (2006). Fine discrimination in the recognition of individual species of phosphatidyl-myo-inositol mannosides from *Mycobacterium tuberculosis* by C-type lectin pattern recognition receptors. J. Immunol. *177*, 1805–1816.

Vergne, I., Chua, J., Singh, S.B., and Deretic, V. (2004). Cell biology of *mycobacterium tuberculosis* phagosome. Annu. Rev. Cell Dev. Biol. *20*, 367–394.

Wieland, C.W., Koppel, E.A., den Dunnen, J., Florquin, S., McKenzie, A.N., van Kooyk, Y., van der Poll, T., and Geijtenbeek, T.B. (2007). Mice lacking SIGNR1 have stronger T helper 1 responses to *Mycobacterium tuberculosis*. Microbes Infect. *9*, 134–141.

Yamasaki, S., Ishikawa, E., Kohno, M., and Saito, T. (2004). The quantity and duration of FcRgamma signals determine mast cell degranulation and survival. Blood *103*, 3093–3101.

Yamasaki, S., Matsumoto, M., Takeuchi, O., Matsuzawa, T., Ishikawa, E., Sakuma, M., Tateno, H., Uno, J., Hirabayashi, J., Mikami, Y., et al. (2009). C-type lectin Mincle is an activating receptor for pathogenic fungus, *Malassezia*. Proc. Natl. Acad. Sci. USA *106*, 1897–1902.

Yamashita, Y., Hoshino, Y., Oka, M., Matsumoto, S., Ariga, H., Nagai, H., Makino, M., Ariyoshi, K., and Tsunetsugu-Yokota, Y. (2013). Multicolor flow cytometric analyses of $CD4^+$ T cell responses to *Mycobacterium tuberculosis*-related latent antigens. Jpn. J. Infect. Dis. *66*, 207–215.

Zhu, L.L., Zhao, X.Q., Jiang, C., You, Y., Chen, X.P., Jiang, Y.Y., Jia, X.M., and Lin, X. (2013). C-type lectin receptors Dectin-3 and Dectin-2 form a heterodimeric pattern-recognition receptor for host defense against fungal infection. Immunity *39*, 324–334.

Clinical Radiology 69 (2014) 758–764

Contents lists available at ScienceDirect

Clinical Radiology

journal homepage: www.clinicalradiologyonline.net

Evaluation of the extent of ground-glass opacity on high-resolution CT in patients with interstitial pneumonia associated with systemic sclerosis: Comparison between quantitative and qualitative analysis

H. Yabuuchi [a,*], Y. Matsuo [b], H. Tsukamoto [c], T. Horiuchi [c], S. Sunami [b], T. Kamitani [b], M. Jinnouchi [b], M. Nagao [b], K. Akashi [c], H. Honda [b]

[a] *Department of Health Sciences, Kyushu University Graduate School of Medical Sciences, Fukuoka, Japan*
[b] *Department of Clinical Radiology, Kyushu University Graduate School of Medical Sciences, Fukuoka, Japan*
[c] *Department of Medicine and Biosystemic Science, Kyushu University Graduate School of Medical Sciences, Fukuoka, Japan*

ARTICLE INFORMATION

Article history:
Received 6 June 2013
Received in revised form
5 March 2014
Accepted 6 March 2014

AIM: To verify whether quantitative analysis of the extent of ground-glass opacity (GGO) on high-resolution computed tomography (HRCT) could show a stronger correlation with the therapeutic response of interstitial pneumonia (IP) associated with systemic sclerosis (SSc) compared with qualitative analysis.

MATERIALS AND METHODS: Seventeen patients with IP associated with SSc received autologous peripheral blood stem cell transplantation (auto-PBSCT) and were followed up using HRCT and pulmonary function tests. Two thoracic radiologists assessed the extent of GGO on HRCT using a workstation. Therapeutic effect was assessed using the change of vital capacity (VC) and diffusing capacity of the lung for carbon monoxide (DLco) before and 12 months after PBSCT. Interobserver agreement was assessed using Spearman's rank correlation coefficient and the Bland–Altman method. Correlation with the therapeutic response between quantitative and qualitative analysis was assessed with Pearson's correlation coefficients.

RESULTS: Spearman's rank correlation coefficient showed good agreement, but Bland–Altman plots showed that proportional error could be suspected. Quantitative analysis showed stronger correlation than the qualitative analysis based on the relationships between the change in extent of GGO and VC, and change in extent of GGO and DLco.

CONCLUSION: Quantitative analysis of the change in extent of GGO showed stronger correlation with the therapeutic response of IP with SSc after auto-PBSCT than with the qualitative analysis.

* Guarantor and correspondent: H. Yabuuchi, Department of Health Sciences, Graduate School of Medical Sciences, Kyushu University, 3-1-1 Maidashi, Higashi-ku, Fukuoka 812-8582, Japan. Tel./fax: +81 92 642 6727.
E-mail address: h-yabu@med.kyushu-u.ac.jp (H. Yabuuchi).

0009-9260/$ – see front matter © 2014 The Royal College of Radiologists. Published by Elsevier Ltd. All rights reserved.
http://dx.doi.org/10.1016/j.crad.2014.03.008

Introduction

Ground-glass opacity (GGO) on high-resolution CT (HRCT) in patients with interstitial pneumonia (IP) is thought to correspond to the presence of active inflammation, and/or the presence of fibrosis below the resolution of HRCT.[1,2] In patients with IP associated with systemic sclerosis (SSc), Wells et al.[3] reported that predominant GGO was often correlated with the presence of inflammation. The extent of GGO has been reported correlate with the histological grade of non-specific IP, the prognosis of idiopathic IP, or the therapeutic response of IP associated with collagen vascular disease.[4–9] Kim et al.[10] revealed that there was a significant reduction in the extent of GGO at follow-up CT and an improvement in Forced Vital Capacity (FVC) that correlated with the extent of reduction in GGO at CT.[10] Wells et al.[11] reported that improvement after treatment is more frequent in patients who have prominent GGO than in those with predominant reticular abnormalities.

Therefore, the extent of GGO is an important factor to predict or monitor therapeutic response to IP associated with collagen vascular disease after immunosuppressive therapy such as corticosteroid, cyclophosphamide, and peripheral blood stem cell transplantation (PBSCT).[12–15] The extent of GGO has been visually scored by semiquantitative systems; however, these systems are limited by the requirement for expert thoracic radiologists and by interobserver variance.[4–9] However, the ratio of low attenuation areas (%LAA) using a commercially available workstation has been used as a quantitative marker to evaluate the severity of pulmonary emphysema.[16,17] Shin et al.[18] evaluated the correlation between quantitative CT indexes, pulmonary function tests, and visual scores of CT in patients with diffuse interstitial lung disease, and reported that the ratio of interstitial lung disease volume ($-500>$ and >-700 HU) significantly correlated with diffusing capacity. They defined interstitial disease volume as the lung volume corresponding to areas of attenuation over -700 HU. However, they used the single cut-off value of -700 HU, and the correlation of quantitative CT indexes and therapeutic or temporal change of IP were not analysed.

Thus, the purpose of the present study was to verify whether quantitative analysis of the extent of GGO on HRCT using a workstation could show a stronger correlation with the therapeutic response of IP associated with SSc after auto-PBSCT compared with qualitative analysis.

Materials and methods

This retrospective study was carried out on 17 consecutive patients (12 women, five men; age 53.2 ± 7.2 years; range 34–63 years) who received PBSCT for refractory IP associated with SSc between November 2004 and January 2009, and who were followed up for at least 12 months using HRCT and pulmonary function tests.

The protocols for the therapy and analysis of CT images were approved by the institutional review board. The inclusion criteria for CT analysis were that patients underwent thin-section CT of the chest within 1 month before PBSCT, with follow-up thin-section CT performed every 6 months after the PBSCT. Patients were excluded from the study when they did not meet both criteria.

CT examination

CT examinations were performed using four or 64 section CT systems (Aquilion 64, Aquilion 4, Toshiba Medical Systems, Ohtahara, Japan; Volume Zoom, Erlangen, Germany). Axial images were obtained from the lung apices to the lung base at full inspiration in the supine position. The parameters for thin-section helical scans using four detector-row CT were 4 × 1 mm detector row width; 5.5 or 6 helical pitch; 2 or 1.25 mm section thickness; 10 mm section interval; 0.5 or 0.75 s rotation time; 200–250 mm field of view; 120 kVp tube voltage; 160–200 mA tube current. For the 64 detector-row CT system, the parameters were 64 × 0.5 mm detector row width; 53 helical pitch; 2 mm section thickness; 10 mm section interval; 0.5 s rotation time; 200–250 mm field of view; 120 kVp tube voltage; 160–200 mA tube current. Images were contiguously reconstructed with 5 mm thickness and were also reconstructed with thin section (1.25 or 2 mm) thicknesses at 10 mm intervals. These images were reconstructed using a high-spatial-frequency algorithm. None of the patients received intravenous contrast medium.

Quantitative analysis

For the quantitative analysis, HRCT examinations of both lungs before and 12 months after PBSCT were undertaken in all patients. A commercially available workstation (Fuji film, Vincent, Tokyo) was used to calculate the extent of GGO. First, the lung field was extracted; then the airway was eliminated from the volume data. When automatic elimination did not work, the airway data was eliminated manually using the region-growing method. The region-growing method is a simple pixel-based image segmentation method. It examines neighbouring pixels of initial "seed points" and determines whether the neighbouring pixel should be added to the region.[19] To calculate the extent of GGO, the percentage of lung volume with attenuation values lower than -500 HU and higher than (-790, -800, -810, -820, -830, -840, -850, -860, -870) HU was calculated relative to the volume of the whole lung. Total lung volumes (TLVs) were calculated by counting pixels corresponding to attenuation values of -1024 to -250 using the same workstation.

Determination of threshold of GGO

One author (H.Y.) selected five areas per patient that were visually regarded as normal lung and five areas visually regarded as GGO in all patients. The same author also selected five areas that were visually regarded as consolidation in each patient for whom consolidation could be detected on HRCT ($n = 5$ of 17). In the region of interest (ROI) settings, small vessels and bronchi were eliminated where possible (ROI size: 10–40 mm^2). Referring to the

scattergram of visually regarded normal lung, GGO, and consolidation (Fig 1), various thresholds were tested to examine the correlation between %GGO and therapeutic effects.

Qualitative analysis

The CT images before and 12 months after PBSCT were retrospectively reviewed by two thoracic radiologists (Y.M. and S.S., 16 and 15 years of experience, respectively). They independently analysed the extent of visual GGO without clinical information or biopsy results. In addition to the extent of GGO, the extents of reticular opacities, honeycombing, and emphysema were also evaluated by the same two observers to confirm that these findings did not show marked change before and after the PBSCT. The thin-section CT images from the lung apices to the lung base section (thickness and interval, 2 or 1.25 mm/10 mm) were used for qualitative analyses. According to the reports of Johkoh et al.[4] and Sumikawa et al.,[5] the extent of GGO was determined by visually estimating the extent in the upper, middle, and lower lung zones in each lung based on the percentage of the lung field that showed each abnormality in each zone (estimated to the nearest 10% of parenchymal involvement). The overall percentage of involvement was obtained by averaging the six zones. The upper zone was defined as the area above the level of the carina; the lower zone as the area below the level of the inferior pulmonary vein; and the middle zone as the area between the upper and lower zones.

Evaluation of therapeutic effect

IP was evaluated by total lung capacity (TLC), vital capacity (VC), %VC, diffusing capacity of the lung for carbon monoxide (DLco) and %DLco measured using a pulmonary function test. These pulmonary function tests were performed based on published guidelines.[20–22] The interval between the pulmonary function test and CT examination was within 2 weeks in all patients. The values obtained by pulmonary function tests were expressed in absolute terms and as a percentage of the predicted value. Predicted values were derived from reference equations, separated by gender with age and height as predicted variables.[20–22] The TLC, VC, %VC, DLco and %DLco were recorded 1 month before and 12 months after PBSCT. Then, the change in VC and DLco was calculated from before to after the treatment. Change in VC was defined the as

Δ VC: VC at 12 months after PBSCT − VC at 1 month before PBSCT.

We also defined the change in DLco as

ΔDLco: DLco at 12 months after PBSCT − DLco at 1 month before PBSCT.

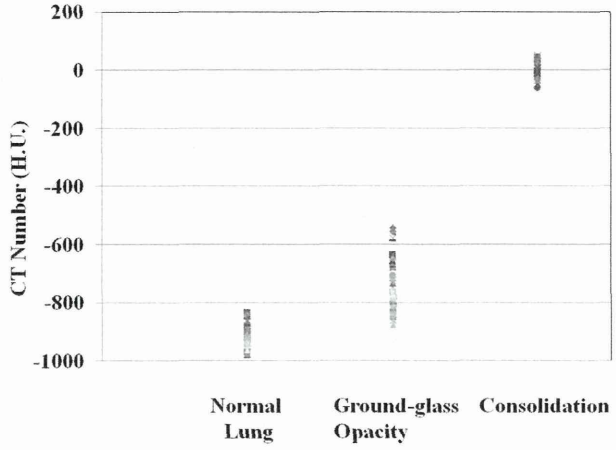

Figure 1 Scattergram of radiodensity in regions of normal lung, GGO, and consolidation as determined visually. The radiodensity ranges of consolidation and GGO were clearly separated; therefore, −500 HU was selected as the threshold between consolidation and GGO. The radiodensity of GGO and that of normal lung overlapped, so various thresholds were tested to find the strongest correlation with therapeutic effects.

Statistical analysis

Interobserver agreement in the assessment of the extent of GGO on qualitative analysis was assessed using Spearman's rank correlation coefficient and the Bland–Altman method. Baseline CT and follow-up CT obtained 12 months after PBSCT in 17 patients (total 34 CT images) were used to assess interobserver agreement. In the Bland–Altman method, the mean value, SD, mean difference, and 95% limits of agreement for the two paired sets of the extent of GGO measurements were analysed. Two potential sources of systemic disagreement (fixed and proportional bias) between the two observers were analysed. Fixed bias means that one observer gives values that are higher or lower than those from the other by a constant amount. Proportional bias means that one observer gives values that are higher or lower than those from the other by an amount that is proportional to the level of the measured variable. When 95% confidence intervals of the mean differences does not include zero, that was regarded as the existence of fixed bias. In addition, correlation coefficients were calculated from the regression analysis Bland-Altman plot to test whether proportional bias existed.[23]

In view of the correlation with the therapeutic response between quantitative and qualitative analysis, Pearson's correlation coefficients were used to evaluate whether change in VC (ΔVC) and DLco (ΔDLco) were correlated with the change in extent of GGO (ΔGGO) 12 months after PBSCT both in quantitative and qualitative analyses. p-Values <0.05 were considered statistically significant.

Results

Determination of threshold of GGO

Fig 1 depicts a scattergram of CT attenuation values for regions of normal lung, GGO, and consolidation, as determined visually. The CT attenuation values for consolidation and GGO were clearly separated; therefore, −500 HU was selected as the threshold between consolidation and GGO. Table 1 shows the relationship between ΔGGO using

Table 1
Relationship between the change of extent of ground-glass opacity using various threshold (Δextent of GGO) and therapeutic effect (ΔVC, ΔDLco).

Threshold (Δextent of GGO)	vs. ΔVC (γ, p-value)	vs. ΔDLco (γ, p-value)
−500 ~ −790	−0.51 ($p = 0.05$)	−0.46 ($p = 0.052$)
−500 ~ −800	−0.54 ($p = 0.03$)[a]	−0.48 ($p = 0.045$)[a]
−500 ~ −810	−0.49 ($p = 0.04$)	−0.47 ($p = 0.0047$)
−500 ~ −820	−0.47 ($p = 0.05$)	−0.47 ($p = 0.047$)
−500 ~ −830	−0.45 ($p = 0.06$)	−0.47 ($p = 0.049$)
−500 ~ −840	−0.42 ($p = 0.08$)	−0.46 ($p = 0.052$)
−500 ~ −850	−0.39 ($p = 0.11$)	−0.41 ($p = 0.09$)
−500 ~ −860	−0.34 ($p = 0.17$)	−0.42 ($p = 0.08$)
−500 ~ −870	−0.29 ($p = 0.24$)	−0.38 ($p = 0.12$)

[a] Threshold showing highest γ value.

various thresholds at quantitative analysis and therapeutic effect (ΔVC, ΔDLco). A threshold between −500 and −800 revealed the best relationship with ΔVC ($r = -0.54$, $p = 0.03$), and ΔDLco ($r = -0.48$, $p = 0.045$), where r stands for Pearson's correlation coefficients.

Raw data of quantitative and qualitative analyses

The range and median values of %GGO before PBSCT by quantitative analysis and qualitative analyses (observer 1 and observer 2) were 16.9–46.8 (30), 3.3–71.7 (30), and 5–65 (25), respectively. The range and median value of % GGO after PBSCT by quantitative analysis and qualitative analyses (observer 1 and observer 2) were 14–31.3 (22.1), 1.7–41.7 (16.7), and 0.5–36 (13.7), respectively. Among 17 patients, GGO and reticular opacities were detected in all patients at pretreatment and post-treatment CT; honeycombing was seen in four patients; and emphysema was seen in one patient. The extent of reticular opacities, honeycombing, and emphysema were about the same before and after the PBSCT. The range and median values of reticular opacities before PBSCT by qualitative analyses (observer 1 and observer 2) were 3–25 (10) and 3–20 (7), respectively. The range and median value of reticular opacities after PBSCT by qualitative analyses (observer 1 and observer 2) were 3–27.5 (10) and 3–25 (8), respectively.

Interobserver agreement in qualitative analysis

Spearman's rank correlation coefficient between observer 1 and observer 2 (Fig 2a) showed good agreement in evaluation of ΔGGO ($r = 0.54$, $p < 0.05$). However, Bland–Altman plots showed that the Pearson r (difference versus mean) was 0.48 ($p < 0.05$; Fig 2b); therefore, proportional error could be suspected.

Comparison between quantitative and qualitative analysis in the correlation with therapeutic effect

Fig 3 shows the relationship between ΔGGO and ΔVC. Qualitative analysis of observer 1 and observer 2 exhibited no significant correlation with ΔVC (observer 1, $r = -0.45$, $p = 0.07$; observer 2, $r = -0.47$, $p = 0.06$). Quantitative analysis revealed a significant and stronger correlation with ΔVC ($r = -0.54$, $p = 0.03$) than those of qualitative analyses. Fig 4 shows the relationship between ΔGGO and ΔDLco. Qualitative analysis of both observers exhibited no significant correlation with ΔDLco (observer 1, $r = -0.28$, $p = 0.28$; observer 2, $r = -0.21$, $p = 0.41$); however, quantitative analysis revealed a significant correlation with ΔDLco ($r = -0.48$, $p = 0.04$).

Fig 5 is a representative case that showed good response after PBSCT. Red areas corresponding to GGO (between −800 and −500 HU) decreased after PBSCT, and quantitative analysis of ΔGGO decreased from 43% to 28%.

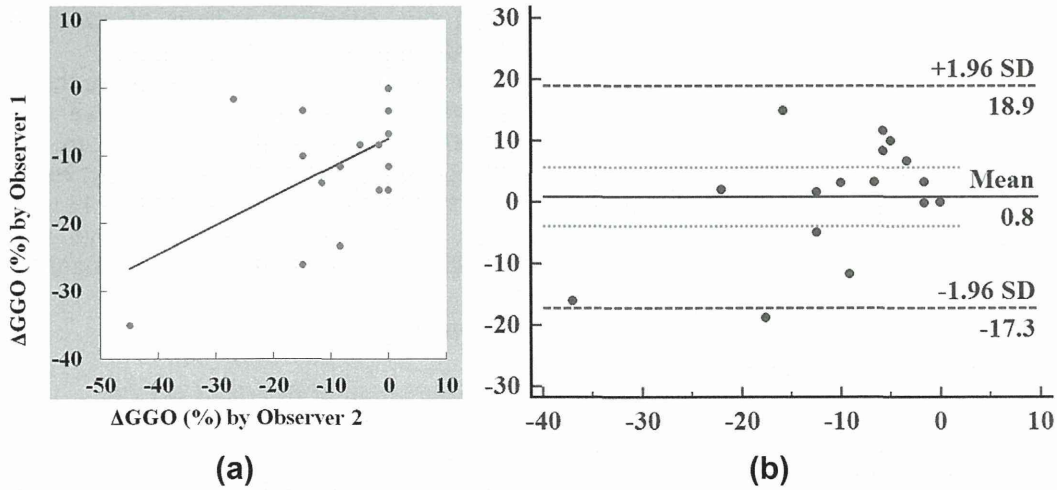

Figure 2 Interobserver agreement in qualitative analysis of ΔGGO using Spearman's rank correlation coefficient (a) and Bland–Altman plots (b). (a) Spearman's rank correlation coefficient between observer 1 and observer 2 shows good agreement in evaluation of ΔGGO ($r = 0.54$, $p < 0.05$). (b) Bland–Altman plots shows that the Pearson r (difference versus mean) was 0.48 ($p < 0.05$) and the 95% CI of average difference (small dotted lines; −3.95 to 5.55) included 0.0; therefore, fixed bias could be denied and proportional error could be suspected.

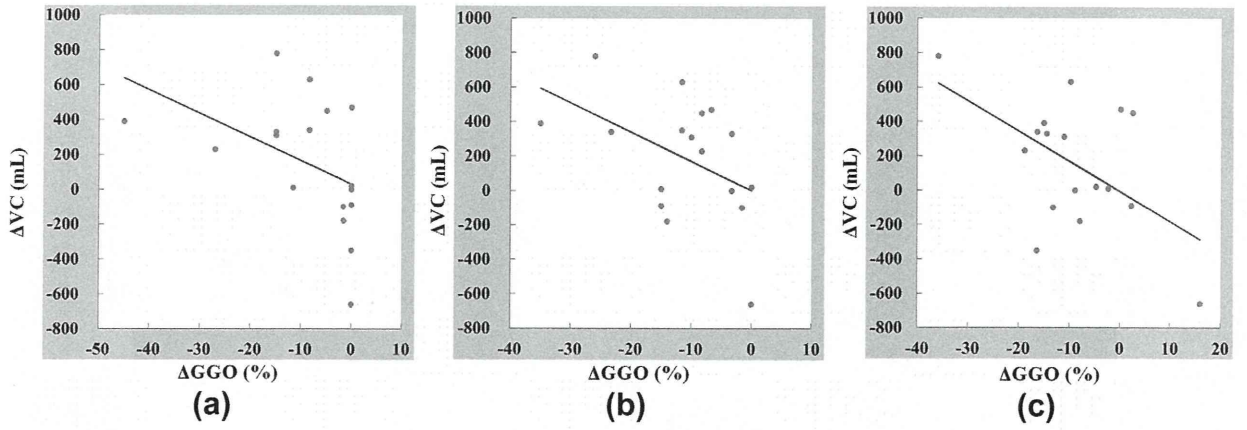

Figure 3 The relationship between ΔGGO and ΔVC. (a) Qualitative analysis of observer 1 exhibits significant correlation with ΔVC ($r = -0.45$, $p = 0.07$). (b) Qualitative analysis of observer 2 also shows significant correlation with ΔVC ($r = -0.47$, $p = 0.06$). (c) Quantitative analysis reveals more significant correlation with ΔVC ($r = -0.54$, $p = 0.03$) than those of qualitative analyses.

Discussion

The results of the present study showed that quantitative analysis of the extent of GGO in IP associated with SSc showed a stronger correlation with therapeutic effects than the qualitative analysis. In past studies on HRCT of IP, a semiquantitative visual scoring system was used to evaluate the extent of disease at CT.[4–9] However, semiquantitative scoring systems are limited by the requirement for expert radiologists and interobserver variance.[4–9] As Bland–Altman plot analysis in the present study showed that proportional error could be suspected in qualitative analysis by two observers, quantitative analysis of the extent of GGO might be able to eliminate observer-dependent bias; here, it resulted in more accurate analysis. It could be a useful method to evaluate the therapeutic change of IP with HRCT.

Regarding the monitoring the activity of IP, pulmonary function tests, including VC or DLco, have been widely used as an indicator of IP activity. Among the various parameters of pulmonary function tests, VC and DLco were selected as therapeutic response markers according to an official American Thoracic Society (ATS)/European Respiratory Society (ERS)/Japanese Respiratory Society (JRS)/Latin American Thoracic Association (ALAT) statement for idiopathic pulmonary fibrosis for monitoring the clinical course of disease of IP.[24]

However, GGO at HRCT has also been thought to be an indicator of the therapeutic response of IP.[25,26] Therefore, assessment of the change in the extent of GGO might affect the judgment of therapeutic response and might influence the therapeutic plan or management.

The results of the present study also showed that the threshold of −500 to −800 HU for GGO revealed the strongest correlation with therapeutic effects. CT attenuation of normal lung parenchyma is reported to range from −800 to −900 HU, although it depends on inspiration or expiration and anatomical location, namely ventral or dorsal portion.[27–29] Therefore, the present threshold of −500 to −800 HU for GGO seems a reasonable range. CT attenuation of lung parenchyma depends on the level of inspiration achieved for the scan; however, this limitation seems to affect both quantitative and qualitative analysis of GGO.

Concerning the thresholds for interstitial lung disease, Shin et al.[18] defined the area with attenuations between

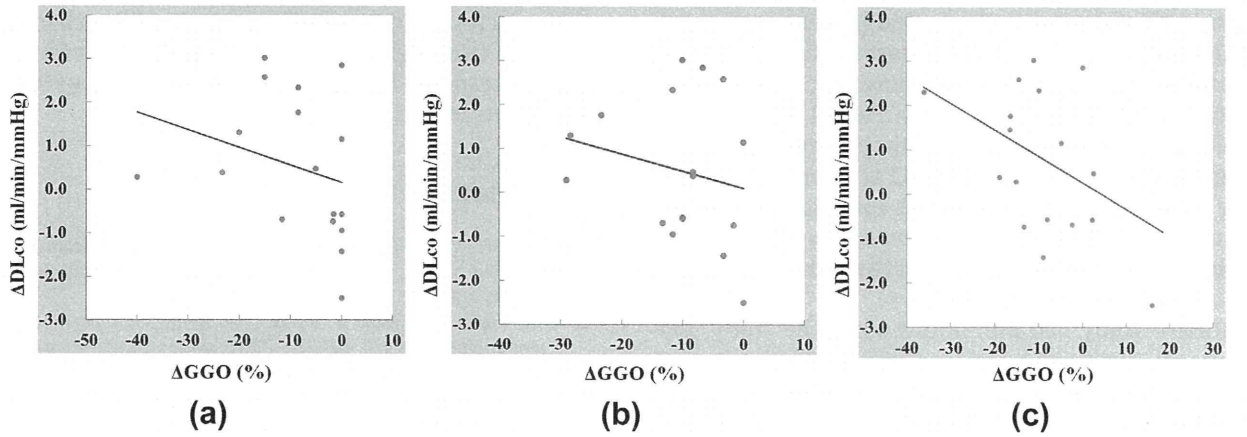

Figure 4 The relationship between ΔGGO and Δ DLco. (a) Qualitative analysis of observer 1 does not exhibit a significant correlation with Δ DLco ($r = -0.28$, $p = 0.28$). (b) Qualitative analysis of observer 2 also shows no significant correlation with ΔDLco ($r = -0.21$, $p = 0.41$). (c) Quantitative analysis reveals significant correlation with ΔDLco ($r = -0.48$, $p < 0.05$).

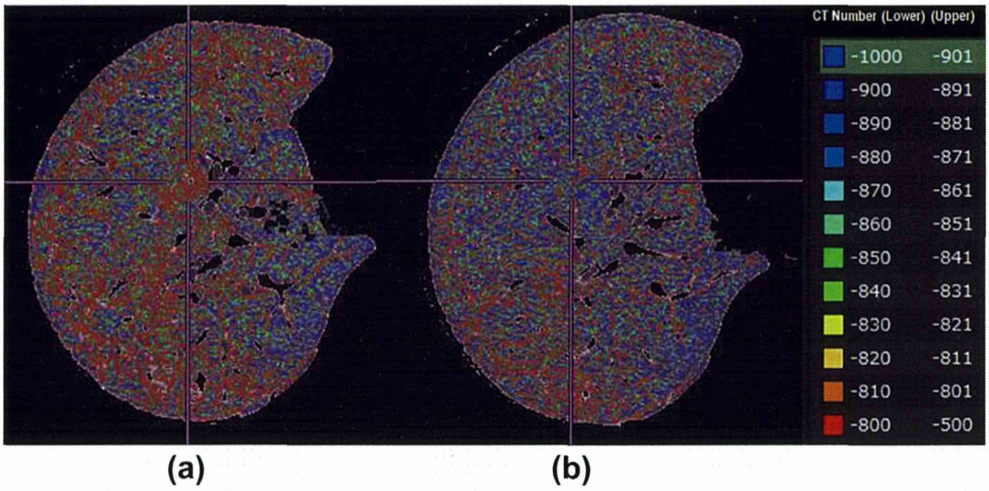

Figure 5 A 48-year-old woman with SSc. (a) CT densitogram indicates areas with radiodensity values over −800 and less than −500 in red. Quantitative analysis of the extent of %GGO before PBSCT is 43%. (b) Areas in red apparently decrease after PBSCT on the CT densitogram. Quantitative analysis of the extent of %GGO 1 year after PBSCT is 28%.

−500 and −700 HU as interstitial lung disease, whereas in the present study the thresholds of −500 and −800 HU were used. CT values were initially analysed in visually normal lung and GGO, and various thresholds between −790 to −870 HU were tested to examine the correlation between %GGO and therapeutic effects, whereas Shin et al. might have included GGO and other abnormalities, such as reticular opacity. Several factors, including small sample size, different CT unit, and background patient populations, might affect the difference in thresholds between these studies.

Yoon et al.[30] also evaluated the usefulness of an automated quantification system (AQS) for evaluating the extent and interval change of fibrotic IP.[30] An AQS that they developed quantified five patterns (GGO, reticular opacity, honeycombing, emphysema, consolidation, and normal lung). Their AQS was comparable with visual assessment for evaluating the extent and the interval change of fibrotic IP, and showed good correlation with pulmonary function test (PFT). The interobserver agreement in assessing the interval change of GGO was poor in their study; this point is consistent with the present study. The present study evaluated GGO only, because this is the most sensitive finding to immunosuppressive therapy in IP; however, this is one of the limitations of the present study. Partial volume averaging of reticular opacity or honeycombing and adjacent air might be counted as the area of GGO at quantitative analysis. The median values of %GGO at quantitative analysis before and after PBSCT in the present study were slightly higher than those at qualitative analysis, this result might support the authors' speculation.

The present study had limitations. First, the study population was relatively small and was limited to patients with IP associated with SSc. In the future, the present method should be tested in patients with idiopathic IP. Second, only the extent of GGO was analysed in the present study; other findings, such as traction bronchiectasis or honeycombing, should be included in the quantitative analysis of future studies. Third, pre-treatment and post-PBSCT images were not directly compared because an expectation bias that the current image must have improved after aggressive therapy could not be eliminated in the reading test. However, this is not the usual method of reading in clinical practice. Fourth, infectious or non-infectious complications could not be strictly excluded based on laboratory findings or clinical history alone in patients with progressive IP. Fifth, in the quantitative analysis the focus was on GGO alone, because this is the most reversible CT finding of IP to immunosuppressive therapy; honeycombing, traction bronchiectasis, and reticular opacity were not analysed using the workstation in the present study. These findings might be less detectable by a computer than by experienced chest radiologists. Sixth, quantitative analysis in the present study was performed by one observer; therefore, it also needs to be validated by interobserver or intra-observer or inter-software variance in a future study. However, this is an initial report to prove the utility of quantitative analysis of the extent of GGO using a workstation to compare qualitative analysis by thoracic radiologists.

In conclusion, quantitative analysis of the change in the extent of GGO showed stronger correlation with the therapeutic response of IP with SSc after auto-PBSCT than qualitative analysis.

References

1. Leung AN, Miller RR, Müller NL. Parenchymal opacification in chronic infiltrative lung diseases: CT–pathologic correlation. *Radiology* 1993;**188**:209–14.
2. Remy-Jardin M, Giraud F, Remy J, et al. Importance of ground-glass attenuation in chronic diffuse infiltrative lung disease: pathologic–CT correlation. *Radiology* 1993;**189**:693–8.
3. Wells AU, Hansell DM, Corrin B, et al. High-resolution computed tomography as a predictor of lung histology in systemic sclerosis. *Thorax* 1992;**47**:508–12.
4. Johkoh T, Müller NL, Colby TV, et al. Nonspecific interstitial pneumonia: correlation between thin-section CT findings and pathologic subgroups in 55 patients. *Radiology* 2002;**225**:199–204.

5. Sumikawa H, Johkoh T, Ichikado K, et al. Usual interstitial pneumonia and chronic idiopathic interstitial pneumonia: analysis of CT appearance in 92 patients. *Radiology* 2006;**241**:258–66.
6. Jeong YJ, Lee KS, Müller NL, et al. Usual interstitial pneumonia and non-specific interstitial pneumonia: serial thin-section CT findings correlated with pulmonary function. *Korean J Radiol* 2005;**6**:143–52.
7. Arakawa H, Yamada H, Kurihara Y, et al. Nonspecific interstitial pneumonia associated with polymyositis and dermatomyositis: serial high-resolution CT findings and functional correlation. *Chest* 2003;**123**: 1096–103.
8. Collins CD, Wells AU, Hansell DM, et al. Observer variation in pattern type and extent of disease in fibrosing alveolitis on thin section computed tomography and chest radiography. *Clin Radiol* 1994;**49**:236–40.
9. Camiciottoli G, Orlandi I, Bartolucci M, et al. Lung CT densitometry in systemic sclerosis, correlation with lung function, exercise test and quality of life. *Chest* 2007;**131**:672–81.
10. Kim EY, Lee KS, Chung MP, et al. Nonspecific interstitial pneumonia with fibrosis: serial high-resolution CT findings with functional correlation. *AJR Am J Roentgenol* 1999;**173**:949–53.
11. Wells AU, Hansell DM, Rubens MB, et al. The predictive value of appearance of thin-section computed tomography in fibrosing alveolitis. *Am Rev Respir Dis* 1993;**148**:1076–82.
12. Tsukamoto H, Nagafuji K, Horiuchi T, et al. A phase I–II trial of autologous peripheral blood stem cell transplantation in the treatment of refractory autoimmune disease. *Ann Rheum Dis* 2006;**65**:508–14.
13. Tyndall A, Passweg J, Gratwohl A. Haemopoietic stem cell transplantation in the treatment of severe autoimmune diseases 2000. *Ann Rheum Dis* 2001;**60**:702–7.
14. Burt RK, Arnold R, Emmons R, et al. Stem cell therapy for autoimmune disease: overview of concepts from the Snowbird 2002 tolerance and tissue regeneration meeting. *Bone Marrow Transplant* 2003;**32**(Suppl 1): S3–5.
15. Nash RA, McSweeney PA, Crofford LJ, et al. High-dose immunosuppressive therapy and autologous hematopoietic cell transplantation for severe systemic sclerosis: long-term follow-up of the US multicenter pilot study. *Blood* 2007;**15**:1388–96.
16. Matsuoka S, Kurihara Y, Yagihashi K, et al. Quantitative assessment of air trapping in chronic obstructive pulmonary disease using inspiratory and expiratory volumetric MDCT. *AJR Am J Roentgenol* 2008;**190**:762–9.
17. Matsuoka S, Yamashiro T, Washnko GR, et al. Quantitative CT assessment of chronic obstructive pulmonary disease. *RadioGraphics* 2010;**30**: 55–66.
18. Shin KE, Chung MJ, Jung MP, et al. Quantitative computed tomographic indexes in diffuse interstitial lung disease: correlation with physiologic tests and computed tomography visual scores. *J Comput Assist Tomogr* 2011;**35**:266–71.
19. Udupa JK. Three-dimensional visualization and analysis methodologies: a current perspective. *RadioGraphics* 1999;**19**:783–806.
20. Macintyre N, Crapo RO, Viegi G, et al. Standardisation of the single-breath determination of carbon monoxide uptake in the lung. *Eur Respir J* 2005;**26**:720–35.
21. Miller MR, Hankinson J, Brusasco V, et al. Standardisation of spirometry. *Eur Respir J* 2005;**26**:319–38.
22. Pellegrino R, Viegi G, Brusasco V, et al. Interpretative strategies for lung function tests. *Eur Respir J* 2005;**26**:948–68.
23. Bland M, Altman DG. Statistical methods for assessing agreement between two methods of clinical measurement. *Lancet* 1986;**1**:307–10.
24. Raghu G, Collard HR, Egan JJ, et al. An official ATS/ERS/JRS/ALAT statement: idiopathic pulmonary fibrosis: evidence-based guidelines for diagnosis and management. *Am J Respir Crit Care Med* 2011;**183**:788–824.
25. Screaton NJ, Hiorns MP, Lee KS, et al. Serial high resolution CT in non-specific interstitial pneumonia: prognostic value of the initial pattern. *Clin Radiol* 2005;**60**:96–104.
26. Akira M, Inoue G, Yamamoto S, et al. Non-specific interstitial pneumonia: findings on sequential CT scans of nine patients. *Thorax* 2000;**55**:854–9.
27. Wegener OH, Koeppe P, Oeser H. Measurement of lung density by computed tomography. *J Comput Assist Tomogr* 1978;**2**:263–73.
28. Robinson PJ, Kreel L. Pulmonary tissue attenuation with computed tomography: comparison of inspiration and expiration scans. *J Comput Assist Tomogr* 1979;**3**:740–8.
29. Rosenblum LJ, Mauceri RA, Wellenstein DE, et al. Density patterns in the normal lung as determined by computed tomography. *Radiology* 1980;**137**:409–16.
30. Yoon RG, Seo JB, Kim N, et al. Quantitative assessment of change in regional disease patterns on serial HRCT of fibrotic interstitial pneumonia with texture-based automated quantification system. *Eur Radiol* 2013;**23**:692–701.

Biol Blood Marrow Transplant 20 (2014) 1968–1974

Biology of Blood and Marrow Transplantation

journal homepage: www.bbmt.org

ASBMT American Society for Blood and Marrow Transplantation

Treatment of Patients with Adult T Cell Leukemia/Lymphoma with Cord Blood Transplantation: A Japanese Nationwide Retrospective Survey

Koji Kato [1,*], Ilseung Choi [2], Atsushi Wake [3], Naokuni Uike [2], Shuichi Taniguchi [3], Yukiyoshi Moriuchi [4], Yasushi Miyazaki [5], Hirohisa Nakamae [6], Eijirou Oku [7], Makoto Murata [8], Tetsuya Eto [9], Koichi Akashi [1], Hisashi Sakamaki [10], Koji Kato [11], Ritsuro Suzuki [12], Takeharu Yamanaka [13], Atae Utsunomiya [14]

[1] *Department of Medicine and Biosystemic Science, Kyushu University Graduate School of Medical Sciences, Fukuoka, Japan*
[2] *Department of Hematology, National Kyushu Cancer Center, Fukuoka, Japan*
[3] *Department of Hematology, Toranomon Hospital, Tokyo, Japan*
[4] *Department of Hematology, Sasebo City General Hospital, Sasebo, Japan*
[5] *Department of Hematology and Molecular Medicine Unit, Atomic Bomb Disease Institute, Nagasaki University Graduate School of Biomedical Science, Nagasaki, Japan*
[6] *Department of Hematology, Osaka City University Graduate School of Medicine, Osaka, Japan*
[7] *Department of Hematology, Kurume University Graduate School of Medicine, Kurume, Japan*
[8] *Department of Hematology, Nagoya University Graduate School of Medicine, Nagoya, Japan*
[9] *Department of Hematology, Hamanomachi Hospital, Fukuoka, Japan*
[10] *Department of Hematology, Tokyo Metropolitan Cancer and Infectious Disease Center, Komagome Hospital, Tokyo, Japan*
[11] *Department of Hematology and Oncology, Children's Medical Center, Japanese Red Cross Nagoya First Hospital, Nagoya, Japan*
[12] *Department of HSCT Data Management/Biostatistics, Nagoya University Graduate School of Medicine, Nagoya, Japan*
[13] *Research Center for Innovative Oncology, National Cancer Center Hospital East, Kashiwa, Japan*
[14] *Department of Hematology, Imamura Bun-in Hospital, Kagoshima, Japan*

Article history:
Received 9 June 2014
Accepted 12 August 2014

Key Words:
Adult T cell leukemia/lymphoma (ATTL)
Cord blood transplantation
Graft-versus-adult T cell leukemia/lymphoma

A B S T R A C T

Allogeneic bone marrow and peripheral blood stem cell transplantations are curative treatment modalities for adult T cell leukemia/lymphoma (ATLL) because of the intrinsic graft-versus-ATLL effect. However, limited information is available regarding whether cord blood transplantation (CBT) induces a curative graft-versus-ATLL effect against aggressive ATLL. To evaluate the effect of CBT against ATLL, we retrospectively analyzed data from 175 patients with ATLL who initially underwent single-unit CBT. The 2-year overall survival (OS) rate was 20.6% (95% confidence interval [CI], 13.8% to 27.4%). A multivariate analysis revealed that the development of graft-versus-host disease (GVHD) was a favorable prognostic factor for OS (hazard ratio, .10; 95% CI, .01 to .94; $P = .044$). Furthermore, the 2-year OS (42.7%; 95% CI, 28.1% to 56.6%) of patients with grade 1 to 2 acute GVHD was higher than that of patients without acute GVHD (24.2%; 95% CI, 11.2% to 39.8%; $P = .048$). However, the cumulative incidence of treatment-related mortality (TRM) was high (46.1%; 95% CI, 38.2% to 53.7%), and early death was particularly problematic. In conclusion, CBT cures patients with ATLL partly through a graft-versus-ATLL effect. However, novel interventions will be required, particularly in the early phase, to reduce TRM and optimize GVHD.

INTRODUCTION

Adult T cell leukemia/lymphoma (ATLL), an aggressive peripheral T cell neoplasm caused by the human T cell lymphotropic/leukemia virus type-1, has an extremely poor prognosis [1]. Intensive chemotherapy and autologous stem cell transplantation have not been shown to improve this prognosis [2,3]. As a curative treatment, allogeneic hematopoietic stem cell transplantation (allo-HSCT) can confer long-term remission via a graft-versus-ATLL effect in a proportion of patients with ATLL [4-7]. Recent reports have demonstrated that allo-HSCT using bone marrow (BM) or peripheral blood stem cells (PBSC) from a related or unrelated donor can effectively treat ATLL, yielding a 3-year overall survival rate

Financial disclosure: See Acknowledgments on page 1973.

* Correspondence and reprint requests: Koji Kato, MD, PhD, Department of Medicine and Biosystemic Science, Kyushu University Graduate School of Medical Science, 3-1-1 Maidashi, Higashi-ku, Fukuoka 812-8582, Japan.
E-mail address: kojikato@intmed1.med.kyushu-u.ac.jp (K. Kato).

http://dx.doi.org/10.1016/j.bbmt.2014.08.012
1083-8791/© 2014 American Society for Blood and Marrow Transplantation.

(OS) of approximately 30% [8-16]. However, patients with ATLL typically lack a suitable HLA-identical sibling donor because both the recipients and donors are typically elderly and because the aggressive ATLL tumor burden reduces the available time to find a suitable unrelated donor within the Japan Marrow Donor Program. Umbilical cord blood, which can serve as an alternative to BM or PBSC as a source of stem cells, has been used primarily to treat children; however, the number of unrelated-donor cord blood transplantation (CBT) procedures used to treat adult patients with ATLL is increasing in Japan. The rapid availability of CBT may provide a great advantage for patients who require urgent allo-HSCT to treat aggressive ATLL [17].

Currently, the outcome of CBT in patients with acute leukemia is comparable to that of other graft sources [18,19]; however, there are few reports on the outcomes of CBT in patients with ATL [20,21]. Moreover, it is difficult to draw firm conclusions regarding the efficacy of this procedure because of the small number of cases. Therefore, to evaluate the role of CBT for ATLL in a larger and more recent cohort, we performed a nationwide retrospective study of patients with ATLL who underwent CBT as the initial allo-HSCT.

PATIENTS AND METHODS

Data Collection

We analyzed nationwide survey data from the Japan Society for Hematopoietic Cell Transplantation regarding patients with ATLL who had undergone an initial CBT between March 2001 and December 2009 (n = 175). This analysis included the patients' clinical characteristics, such as the age at transplantation, gender, disease status at transplantation, date of transplantation, time from diagnosis to transplantation, conditioning regimens, and number of infused cells. The number of mismatches was counted with respect to HLA-A, HLA-B (low-resolution typing), and DRB1 (high-resolution typing). The present study was approved by the data management committees of the Japan Society for Hematopoietic Cell Transplantation as well as the institutional ethics committee of the Kyushu University Graduate School of Medical Sciences.

Definitions

OS was defined as the time from transplantation until death, and patients who remained alive at the time of the last follow-up were censored. The causes of death were reviewed and categorized as either ATLL-related or transplantation-related mortality (TRM). *ATLL-related mortality* was defined as death caused by a relapse or progression of ATLL, whereas *TRM* was defined as any death related to transplantation other than ATLL-related mortality, according to the judgment of each institution. The patients were divided into 2 groups according to the conditioning regimen: full-intensity conditioning (FIC) and reduced-intensity conditioning (RIC). FIC and RIC were defined according to the proposals of Giralt et al. [22] and Bacigalupo et al. [23], respectively, with slight modifications. In the present study, conditioning regimens that included ≥5 Gy of total body irradiation (TBI) in a single fraction or ≥8 Gy of TBI in multiple fractions, oral busulfan (BU) at >8 mg/kg, intravenous BU at >6.4 mg/kg, or melphalan (Mel) at >140 mg/m^2 were considered FIC; all others were classified as RIC.

Statistical Analysis

Descriptive statistics were used to summarize the variables related to patient demographics and transplantation characteristics. The probability of the OS time was estimated according to the Kaplan-Meier method. To evaluate the influences of confounding factors on acute graft-versus-host disease (GVHD) and survival, the log-rank test and proportional hazards modeling were used for the univariate and multivariate analyses, respectively. The Cox proportional hazard model was used for the multivariate analyses of OS in which all independent variables were incorporated in the model, followed by the use of a stepwise selection method [24]. Fine and Gray proportional hazard modeling was used to estimate the effects of the same variables used in the multivariate analysis for OS on the cumulative incidence rates of TRM and ATLL-related mortality [25,26]. In these regression models, the occurrence of GVHD was treated as a time-dependent covariate [27]. In the analysis of acute GVHD, patients were assigned to the "no acute GVHD group" at the time of transplantation and transferred to the "acute GVHD group" at the onset of the maximum grade of acute GVHD. The landmark method was used to evaluate the effects of GVHD on OS and the cumulative incidence of disease-associated and treatment-related deaths among patients who remained alive at 60 days for acute GVHD and at 100 days for chronic GVHD after transplantation. Factors associated with at least borderline significance ($P \leq .10$) in the univariate analysis were subjected to a multivariate analysis using a backward stepwise covariate selection. All P values were 2-tailed, and P values ≤.05 were considered statistically significant. All statistical analyses were performed using EZR (Saitama Medical Center, Jichi Medical University), a graphical user interface for R (The R Foundation for Statistical Computing, version 2.13.0) [28].

RESULTS

Patient Characteristics

The characteristics of 175 ATLL patients who received a single CBT are shown in Table 1. The median age at CBT was 55 years (range, 27 to 79 years). The cohort comprised 70 women and 105 men with the following ATLL statuses at CBT: complete remission (CR; n = 50), not in CR (n = 116), and unknown (n = 9). The conditioning regimen intensity was classified as FIC in 63 (36%) patients and RIC in 128 (62%) patients. FIC was further subdivided into 2 groups as follows: TBI (n = 47) or non-TBI (n = 15). RIC was also subdivided into 3 groups as follows: fludarabine (Flu) + Mel (n = 75), Flu + BU (n = 15), and other types (n = 15). Cyclosporine and tacrolimus were administered for prophylaxis to 90 (51%) and 77 patients (44%), respectively. Cyclosporine-based prophylaxis was subdivided into 3 groups as follows: (1) cyclosporine

Table 1
Patient Characteristics at Cord Blood Transplantation

Variables	No. of Patients (n = 175)
Age at transplantation, median (range), yr	55 (27-79)
Gender	
Male	105
Female	70
Disease status at transplantation	
CR	50
Not in CR	116
Unknown	9
Conditioning regimen	
FIC	63
RIC	108
Unknown	4
GVHD prophylaxis	
Cyclosporine-based	90
Tacrolimus-based	77
Unknown	8
Time from diagnosis to transplantation, d	
<200	94
≥200	75
Unknown	6
Year of transplantation	
<2005	71
≥2005	104
HLA matching*	
0 mismatched loci	5
1 mismatched locus	36
2 mismatched loci	73
≥3 mismatched loci	42
Unknown	19
ABO matching	
Matched	56
Minor mismatched	49
Major mismatched	69
Unknown	1
Nucleated cells infused per 10^7/kg, median (range)	2.58 (.36-5.34)
CD34-positive cells infused per 10^5/kg, median (range)	.85 (.07-5.39)

* Number of mismatches was counted among HLA-A, -B (low-resolution typing), and DRB1 (high-resolution typing).